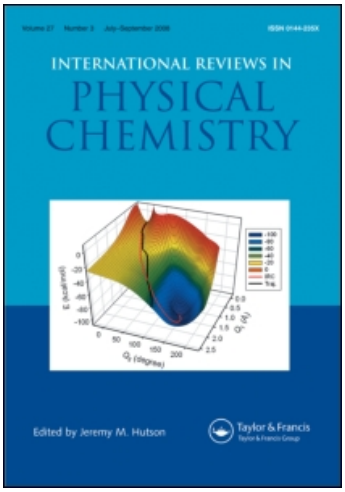

International Reviews in Physical Chemistry
Publication details, including instructions for authors and subscription information:
http://www.informaworld.com/smpp/title~content=t713724383

Theoretical study of the nitrous acid conformers: Comparison of theoretical and experimental structures, relative energies, barrier to rotation and vibrational frequencies

George R. De Mare; Yahia Moussaoui

Online publication date: 26 November 2010

To cite this Article De Mare, George R. and Moussaoui, Yahia(1999) 'Theoretical study of the nitrous acid conformers: Comparison of theoretical and experimental structures, relative energies, barrier to rotation and vibrational frequencies', International Reviews in Physical Chemistry, 18: 1, 91 — 117
To link to this Article: DOI: 10.1080/014423599230017
URL: http://dx.doi.org/10.1080/014423599230017

INTERNATIONAL REVIEWS IN PHYSICAL CHEMISTRY, 1999, VOL. 18, NO. 1, 91–117

Theoretical study of the nitrous acid conformers: comparison of theoretical and experimental structures, relative energies, barrier to rotation and vibrational frequencies

GEORGE R. DE MARÉ†

Laboratoire de Chimie Physique Moléculaire, Faculté des Sciences, CP160/09, Université Libre de Bruxelles, 50 avenue F.-D. Roosevelt, B-1050 Brussels, Belgium

and YAHIA MOUSSAOUI

Laboratoire de Physico-chimie Quantique, Institut de Chimie, Université des Sciences et de la Technologie Houari Boumediene, BP 32, El-Alia, 16111 Bab-Ezzouar, Algiers, Algeria

The experimental and theoretical literature data for the *trans* and *cis* conformers of nitrous acid (HONO) are augmented by additional Hartree–Fock (HF), Møller–Plesset second-order perturbation (MP2), Møller–Plesset fourth-order perturbation (MP4) and density functional (B3LYP) computations. The latter yield optimized theoretical parameters and vibrational frequencies that are closest to the best experimental values. Adding diffuse functions to a given basis set lowers the energy of the *trans* conformer relative to the *cis* at all levels of theory utilized in this work. There have been no convincing assignments of infrared (IR) spectral bands to the O–N=O (ν_3) and H–O–N (ν_5) bending modes of *cis*-HONO, both of which are predicted to have very low intensities. Although IR spectral features about 40 cm^{-1} below ν_3 for *trans*-HONO has been tentatively assigned to ν_3 of *cis*-HONO, calculations with unscaled and scaled quantum-mechanical force fields invert this order. If these predictions are correct, ν_3 of *cis*-HONO would fall in the spectral region around 1300 cm^{-1}, where a number of other compounds containing N and O atoms have IR bands (N_2O, N_2O_4, etc.) and make it difficult to observe. The frequency calculations for *cis*-HONO, with all the unscaled HF force fields, yield $\nu_5 > \nu_6$ (the torsional mode). The situation is reversed for all the frequency calculations with the unscaled B3LYP and MP force fields. Transferring the scale factors obtained for the *trans*-HONO conformer HF/6-311G** force field to the corresponding force field of *cis*-HONO yields $\nu_5 = 590$ cm^{-1} and $\nu_6 = 673$ cm^{-1}, a very good indication that ν_5 is indeed at a lower frequency than ν_6 for the *cis* conformer.

1. Introduction

Nitrous acid reacts with deoxyribonucleic acid (DNA), converting amino functional groups to carbonyl groups and causing interstrand cross-linking which is generally believed to be toxic or even lethal to cells (for leading references see [1]). Melvin and Wulf [2, 3] observed spectral features of nitrous acid in the gas phase in the early 1930s when they studied the ultraviolet (UV) spectra of mixtures of NO, NO_2 and water. This method of producing nitrous acid proved to be very important in subsequent studies of its physical properties. Thus, D'Or and Tarte, [4, 5], Tarte [6] and Jones *et al.* [7], in independent seminal studies on the infrared (IR) spectra of gaseous mixtures of various amounts of NO, NO_2 and light or heavy water, showed

† Author for correspondence. Email: gdemare@ulb.ac.be

International Reviews in Physical Chemistry ISSN 0144-235X print/ISSN 1366-591X online © 1999 Taylor & Francis Ltd
http://www.tandf.co.uk/JNLS/rpc.htm http://www.taylorandfrancis.com/JNLS/rpc.htm

that there is an equilibrium between *s-trans* and *s-cis* conformers of nitrous acid (hereafter denoted by *t*-HONO and *c*-HONO respectively). The isotopic shifts due to deuteration permitted positive identification of some of the absorption bands arising from both of the nitrous acid conformers in the complex equilibrium mixtures [4–7]. Nitrous acid is thus one of the smallest molecules showing rotational isomerism. (The C_{2v} isomer, HNO_2, is higher in energy [8, 9] and probably exists only as a transient species [9]).

Besides the above-mentioned equilibrium, the formation of nitrous acid is observed under a wide variety of conditions. The following are given only as examples because they have been important in studies of the properties of nitrous acid.

(*a*) In low-temperature matrices it is a product of the photolysis of nitric acid [9, 10], of the photolysis of mixtures of ammonia and oxygen [11], of the photolysis of mixtures of hydrazoic acid and oxygen [12–15] and of the reaction of NO_2 with hydrogen atoms formed by the vacuum UV photolysis of CH_4, H_2O or HCl [16].

(*b*) It is formed in solution by the reaction of sodium nitrite with an acid [17–19], that is

$$2NaNO_2 + H_2SO_4 \rightarrow Na_2SO_4 + 2HONO \quad (1)$$

(and also by the reaction of NO_x on H_2O [20] or H_2SO_4–H_2O [21] surfaces). The HONO concentrations in the solution and above it (gas phase) depend on the experimental conditions [17–21].

(*c*) It is formed by the 'thermal decomposition' of ammonium nitrite (for examples see [22–25]):

$$NH_4NO_2(s) \leftrightarrow NH_3(g) + HONO(g). \quad (2)$$

The equilibrium pressure of HONO at 298 K is reported to be about 0.04 mbar [22–25] and the HONO concentration 'remained practically constant on a time scale of 100 s' [22]. However, the reversible surface-catalysed reaction (or eventually the bimolecular gas phase reaction)

$$2HONO \leftrightarrow H_2O + NO + NO_2 \quad (3)$$

will inevitably occur, leading to the destruction of HONO and contamination by other nitrogen-containing compounds [26, 27].

(*d*) What could be the most important recent development for future experimental studies of the properties of nitrous acid in the gas phase is the observation that nearly pure initial concentrations of gaseous nitrous acid (greater than 99.5% ; absence of other nitrogen-containing compounds) can be obtained by flowing gaseous HCl over solid sodium nitrite [28, 29]:

$$HCl(g) + NaNO_2(s) \leftrightarrow NaCl(s) + HONO(g). \quad (4)$$

The experimental conditions again determine the importance of reaction (3).

The experiments performed on HONO in low-temperature matrices using Fourier transform infrared (FTIR) spectroscopy have revealed interesting features such as doubling of bands due to occupation of different sites in the matrices [10, 11, 15, 23, 24] and the formation of 1 : 1 complexes of the HONO conformers with such diverse molecules as NH_3 [22, 23], N_2 [24], CO [24], C_6H_6 [25] and HNO_3 [25].

Nitrous acid is reactive in the gas phase, in solutions and on surfaces [30, 31]. It is an important pollutant in the stratosphere (enhancing production of chlorine atoms through the conversion of HCl to ClNO on ice crystals or other particulates [32]) and

Table 1. Experimental data (mode (symmetry species), approximate description) for the fundamental vibrational frequencies of *c*-HONO in the gas phase and in low-temperature matrices. (In this and the following tables the quoted uncertainties in the last digits of the experimental data are given in parentheses. They are one standard deviation (1σ) except where the notation ($x\sigma$) is given in the corresponding footnote.)

Method, medium	ν_1(a′), O–H stretch (cm^{-1})	ν_2(a′), N=O stretch (cm^{-1})	ν_3(a′), N–O–H bend (cm^{-1})	ν_4(a′), N–O stretch (cm^{-1})	ν_5(a′), O=N–O bend (cm^{-1})	ν_6(a″), N–O torsion (cm^{-1})
FTIR, gas phase	3426.196 33(17)[a], 3426.218(6)[c]	1640.518 65(22)[a]	(≈ 1292)[b]	851.943 064(31)[a], 851.942 93(56)[d]	—	638.5(5)[c], 639.8[b]
Laser Stark spectroscopy		1640.517(1)[e]	—	—	—	—
Tunable diode laser, gas phase	—	—	—	851.942 54(18)[f]	—	—
IR, gas phase[g]	3424	1640 (m)	1261 (w)	853 (s)	608 (w)	638 (m)
IR, Ar matrices, 4k and 14 K[h]	3412	1633	1265	850	610	637
FTIR, NH_3–O_2–Ar matrix, 4.2 K[i]	—	1632.6	1263.3–1259.4	849.6–843.8	608.0–605.1	639.9–636.0
FTIR, Ar matrix, 20 K[j]	3412.4–3410.7	1634.0–1632.8	—	853.1–850.2	—	638.4
FTIR, N_2 matrix, 4.2 K[k]	3404.0	1629.9	—	869.4	—	—
IR, N_2 matrix, 20 K[l]	3410 (3408[m])	1633	—	865	—	658
FTIR, N_2 matrix, 12 K[n]	3406.3	1632.7–1630.5	—	871.0	—	—
IR, solid, −190 °C[g]	—	1611 (s)	—	857 (m)	721 (m)	518 (m)

[a] From [41, 50]. [b] From [4], low resolution IR. [c] From [46]. [d] From [45]; 10σ for the band origins. [e] From [51]; 3σ. [f] From [47]; 2σ. [g] From [49]. The solid is derived by freezing the equilibrium gas-phase mixture obtained at 25 °C. [h] From [16]. Produced by photolysis of H_2O–NO_2–Ar matrices or simultaneous photolysis of H_2 and deposition of either HCl–NO_2 or CH_4–NO_2 mixtures. The band assigned to *c*-HONO in this paper probably belong to ν_3 *t*-HONO (see text). [i] From [11]. Produced by irradiation of the matrix with the 184.9–253.7 nm mercury lines. The bands assigned to *c*-HONO in this paper probably belong to ν_3 *t*-HONO (see text). [j] From [23, 24]. [k] From [9]. Weak bands corresponding to *c*- and *t*-HONO were observed after photolysis of HNO_3 in Ar matrices only when the matrices were doped with O_2. The photolyses of HNO_3 in N_2, Ar and O_2–Ar matrices all revealed bands attributed to the C_{2v} HNO_2 isomer. [l] From [12]. [m] From [15]. [n] From [10].

Table 2. Experimental data (mode (symmetry species), approximate description) for the fundamental vibrational frequencies of *t*-HONO in the gas phase and in low-temperature matrices.

Method, medium	ν_1(a′), O–H stretch (cm^{-1})	ν_2(a′), N=O stretch (cm^{-1})	ν_3(a′), N–O–H bend (cm^{-1})	ν_4(a′), N–O stretch (cm^{-1})	ν_5(a′), O=N–O bend (cm^{-1})	ν_6(a″), N–O torsion (cm^{-1})
FTIR, gas phase	3590.770 35(11)[a], 3590.711(8)[c]	1699.760 15(13)[a], 1699.800(10)[c]	1263.207 05(4)[a], 1263.183(5)[c]	790.117 060(32)[a], 790.116 81(54)[b]	595.620 23(105)[b]	543.879 80(85)[b]
Tunable diode laser, gas phase	—	1699.758 2(11)[d]	1263.206 81(25)[e]	—	—	—
IR, gas phase[f]	3588 (m)	1699 (*s*)	1265 (s)	791 (s)	593 (s)	540 (m)
FTIR, Ar matrix, 20 K[g]	3572.6–3568.5	1689.1–1688.0	1265.8–1263.9	800.4–796.6	608.7	549.4–548.2
FTIR, N_2 matrix, 4.2 K[h]	3510.9	1677.6	1293.7	816.4	—	—
IR, N_2 matrix, 20 K[i]	3558 (3552[j])	1684	1298	815	625	583
FTIR, N_2 matrix, 12 K[k]	3517.8	1681.5–1680.4	1295.7–1294.9	812.6	—	—
IR, solid, −190 °C[f]	3512 (m)	1635 (s)	1421 (s)	801 (m)	702 (m)	499 (w)

[a] From [41, 42]. [b] From [45]; 5σ for the band origins. [c] From [46]. [d] From [47]; 2σ. [e] From [48]; 2σ. [f] From [49]. The solid is derived by freezing the equilibrium mixture obtained at 25 °C. [g] From [23, 24]; ν_3 only undergoes a very small frequency shift in the Ar matrix. [h] From [9]. Weak bands corresponding to *c*- and *t*-HONO were observed after photolysis of HNO_3 in Ar matrices only when the matrices were doped with O_2. The photolyses of HNO_3 in N_2, Ar, and O_2–Ar matrices all revealed bands attributed to the C_{2v} HNO_2 isomer. [i] From [12]. [j] From [15]. [k] From [10].

Table 3. Experimental bond lengths and bond angles for the nitrous acid conformers.

	r(H–O) (Å)	r(O–N) (Å)	r(N=O) (Å)	∠ (H–O–N) (degrees)	∠ (O–N=O) (degrees)	References
t-HONO						
r_e^a	0.954(5)	1.433(5)	1.163(5)	102.1(3)	110.7(1)	[52]
r_s^b	0.958(5)	1.432(5)	1.170(5)	102.1(5)	110.7(5)	[52, 53]
$\langle r \rangle^c$	0.959(5)	1.442(5)	1.169(5)	102.1(3)	110.6(1)	[52]
r_z^d	0.9472(28)	1.4413(20)	1.1731(22)	102.07(28)	110.45(22)	[54]
	0.98	1.46	1.20	〈105〉	118	[7]
c-HONO						
r_s^b	0.982(5)	1.392(5)	1.185(5)	104.0(7)	113.6(7)	[52, 53]
$\langle r \rangle^c$	0.989(5)	1.399(5)	1.186(5)	103.9(3)	113.6(1)	[52]
r_z^d	0.9753(34)	1.3966(61)	1.1901(54)	104.39(44)	113.48(32)	[54]
	0.98	1.46	1.20	〈103〉	114	[7]

[a] Equilibrium structure estimated using model cubic force field. [b] Substitution structures. [c] Average structures with shrinkage corrections. [d] Average structures without shrinkage corrections.

in the atmosphere (enhancing oxidation processes in the early morning air through photolytic production of OH radicals [17–21, 28, 33–36]). Staffelbach and Neftel [36] stated that their measurements of HONO concentrations in the Po valley air are puzzling: 'If the measurements are right it would mean that about 25% of the OH concentration is due to HONO photolysis and that the contribution of HONO to the odd-H production is about one third.' It is also interesting to note that Matsumoto [37] reported recently that nitrous acid concentrations in the air in Nara, Japan, were higher than those of nitric acid in winter and vice versa in summer (see also [38]). This inversion is probably a consequence of a higher photolysis rate of nitrous acid in the summer.

For the above reasons, the properties of the nitrous acid conformers (geometries, fundamental frequencies, relative stabilities, reactivities, etc.) have been the object of numerous experimental [4–7, 9–26, 29, 32–59] and theoretical studies [8, 22–25, 27, 60–77]. In spite of all this attention, there are still unanswered questions concerning the fundamental vibrational frequencies ν_3 and ν_5 of *c*-HONO (see table 1 and [39–41] and references cited therein), the relative stabilities of the two conformers, and the height of the rotational barrier between them in the gas phase. Note, however, that all the ground-state fundamental vibrational frequencies of *t*-HONO in the gas phase have been measured to five or more significant figures (table 2). The lack of reliable experimental values for all the fundamental frequencies of *c*-HONO has prevented the determination of an experimental equilibrium (r_e) structure for this species (see [52] and table 3).

An important experimental difficulty for gas-phase work lies in the fact that stable equilibrium concentrations of the *t*-HONO and *c*-HONO conformers can only be obtained as trace components in a complex mixture with water, NO, NO_2, N_2O_3, N_2O_4 and a trace of nitric acid [4–7, 30, 31, 39, 41, 55, 56]. (See [55] for an IR spectrum of the gas-phase mixture from 700 to 3800 cm^{-1}.) Whereas increasing the temperature of the gaseous mixture increases the concentration of *c*-HONO relative to that of *t*-HONO in the equilibrium mixtures, it also decreases the total nitrous acid concentration [4–7, 56].

Whether the method of preparing nearly pure nitrous acid by reaction (4) can be

Table 4. *t*-HONO: theoretical bond lengths, bond angles, dipole moments μ, ZPEs and energies of the optimized structure.

Method/basis	r(H–O) (Å)	r(O–N) (Å)	r(N=O) (Å)	∠(H–O–N) (degrees)	∠(O–N=O) (degrees)	μ (D)	ZPE (kJ mol^{-1})	ΔE (hartrees)	References
HF/4-31G	0.9539	1.3995	1.1665	107.91	111.38	2.80	56.6	−204.311914	[60–63][a]
HF/4-31G*	0.9514	1.3479	1.1513	105.24	111.33	2.58	—	−204.443577	[62–64]
HF/4-31G**	0.9462	1.3468	1.1515	105.51	111.37	2.59	—	−204.450187	[a]
HF/6-31G	0.9531	1.3873	1.1712	108.41	111.59	2.88	57.3	−204.521940	[63][a]
HF/6-31G*	0.9508	1.3465	1.1532	105.37	111.37	2.62	—	−204.637676	[63, 65, 66][a]
HF/6-31G**	0.9469	1.3455	1.1534	105.57	111.40	2.62	60.8	−204.644011	[62–64][a]
HF/6-31 +G**	0.9475	1.3436	1.1525	105.81	111.74	2.67	60.5	−204.652357	[66][a]
HF/6-31 ++G**	0.9476	1.3436	1.1525	105.80	111.74	2.67	—	−204.652493	[a]
HF/6-311G**	0.9438	1.3435	1.1436	105.33	111.74	2.55	60.8	−204.700158	[67]
HF/6-311 +G**	0.9450	1.3421	1.1438	105.64	111.93	2.60	—	−204.706851	[a]
HF/6-311 ++G**	0.9449	1.3421	1.1437	105.63	111.93	2.60	60.5	−204.706922	[62][a]
HF/6-31 +G(3df,2p)	0.9445	1.3412	1.1452	105.58	111.83	2.49	60.6	−204.679991	[a]
B3LYP/6-31G**	0.9724	1.4266	1.1787	102.35	110.62	2.16	53.5	−205.700291	[a]
B3LYP/6-311G**	0.9678	1.4331	1.1663	102.29	111.03	2.06	53.3	−205.761769	[a, b]
B3LYP/6-311 ++G**	0.9694	1.4326	1.1655	102.94	111.15	2.13	52.9	−205.771766	[a]
MP2-FU/4-31G**	0.9700	1.4232	1.1942	101.61	110.34	2.49	—	−204.991485	[a]
MP2-FU/6-31G**	0.9710	1.4232	1.1964	101.71	110.32	2.52	53.1	−205.184403	[a]
MP2-FU/6-31 ++G**	0.9735	1.4303	1.1937	102.10	110.57	2.53	52.2	−205.203077	[a]
MP2-FC/6-311G**	0.9652	1.4155	1.1804	101.22	110.92	2.44	53.4	−205.274580	[67][b]
MP2-FU/6-311G**	0.9645	1.4132	1.1797	101.26	110.96	2.45	53.5	−205.330675	[a]
MP2-FU/6-311 +G**	0.9678	1.4182	1.1786	101.95	111.04	2.48	52.7	−205.344259	[a]
MP2-FC/6-311 ++G**	0.9682	1.4204	1.1792	101.87	111.00	2.48	52.6	−205.287770	[a]
MP2-FU/6-311 ++G**	0.9677	1.4181	1.1786	101.93	111.04	2.48	52.7	−205.344362	[a]
MP4SDTQ-FC/6-31G**	0.9717	1.4492	1.1988	101.47	110.35	2.43	52.1	−205.207493	[a]
MP4SDTQ-FC/6-311 +G**	0.9698	1.4522	1.1817	101.52	110.97	2.38	51.3	−205.323237	[a]

[a] This work. [b] The optimized geometries reported in [27, 74] are almost within rounding-off errors of these results.

Table 5. *c*-HONO: theoretical bond lengths, bond angles, dipole moments μ, ZPEs and energies of the optimized structure.

Method/basis	r(H–O) (Å)	r(O–N) (Å)	r(N=O) (Å)	∠(H–O–N) (degrees)	∠(O–N=O) (degrees)	μ (D)	ZPE (kJ mol^{-1})	ΔE (hartrees)	References
HF/4-31G	0.9646	1.3776	1.1773	111.61	113.94	1.80	—	+2.68	[60–63]
HF/4-31G*	0.9604	1.3280	1.1591	107.41	113.73	1.57	—	−6.60	[62–64]
HF/4-31G**	0.9546	1.3269	1.1595	107.64	113.72	1.59	—	−6.26	[a]
HF/6-31G	0.9639	1.3678	1.1818	112.15	114.02	1.85	57.0	+3.48	[63][a]
HF/6-31G*	0.9596	1.3274	1.1612	107.62	113.73	1.60	—	−5.94	[63, 65, 66]
HF/6-31G**	0.9553	1.3263	1.1614	107.78	113.73	1.61	61.1	−5.64	[62–64][a]
HF/6-31 +G**	0.9557	1.3264	1.1609	108.41	113.92	1.68	—	−1.57	[a]
HF/6-31 ++G**	0.9558	1.3264	1.1608	108.40	113.92	1.67	—	−1.65	[a]
HF/6-311G**	0.9527	1.3244	1.1521	107.93	113.97	1.57	60.9	−3.38	[a]
HF/6-311 +G**	0.9534	1.3247	1.1523	108.49	114.09	1.65	—	+0.64	[a]
HF/6-311 ++G**	0.9534	1.3247	1.1523	108.47	114.09	1.65	60.5	+0.61	[62][a]
HF/6-31 +G(3df,2p)	0.9530	1.3243	1.1536	108.05	114.10	1.60	60.5	−0.61	[a]
B3LYP/6-31G**	0.9834	1.3851	1.1916	105.43	113.22	1.56	53.6	−3.76	[a, b]
B3LYP/6-311G**	0.9795	1.3884	1.1804	105.86	113.65	1.52	53.2	−1.00	[a]
B3LYP/6-311 ++G**	0.9801	1.3916	1.1794	106.80	113.81	1.61	52.6	+4.50	[a]
MP2-FU/4-31G**	0.9805	1.3845	1.2070	104.11	112.76	1.46	—	−5.65	[a]
MP2-FU/6-31G**	0.9813	1.3853	1.2093	104.35	112.77	1.47	53.6	−4.75	[a]
MP2-FU/6-31 ++G**	0.9832	1.3925	1.2074	105.41	113.07	1.52	—	+1.74	[a]
MP2-FC/6-311G**	0.9766	1.3773	1.1938	104.20	113.18	1.44	53.7	−1.79	[67][b]
MP2-FU/6-311G**	0.9761	1.3753	1.1930	104.23	113.20	1.44	—	−1.83	[a]
MP2-FU/6-311 +G**	0.9780	1.3811	1.1921	105.36	113.43	1.51	—	+4.63	[a]
MP2-FC/6-311 ++G**	0.9784	1.3831	1.1928	105.30	113.41	1.51	52.7	+4.57	[a]
MP2-FU/6-311 ++G**	0.9780	1.3809	1.1921	105.34	113.44	1.51	52.8	+4.53	[a]
MP4SDTQ-FC/6-31G**	0.9814	1.4064	1.2139	103.98	112.70	1.42	52.5	−4.70	[a]
MP4SDTQ-FC/6-311 +G**	0.9793	1.4081	1.1976	104.86	113.35	1.45	—	+4.63	[a]

[a] This work. [b] The optimized geometries reported in [27, 74] are almost within rounding-off errors of these results.

used to obtain more accurate measurements of its physical properties remains to be seen (the line strength measurements of *t*-HONO near 1255 cm^{-1} depend on the accuracy of the calculation of the relative conformer populations and thus on their relative energies [28]).

The main objectives of the present paper are firstly to give a fairly comprehensive review of the literature on the physical properties of the HONO conformers (geometries, relative energies, fundamental frequencies, etc.) in their ground electronic state and secondly to provide some new theoretical results. The extensive literature on the photolysis and on the UV and visible spectroscopy of nitrous acid is not discussed. To simplify the presentation further, the data on the deuterated and nitrogen-15 isotopomers will not be considered in detail in this work.

2. Method

Complete optimizations of the molecular geometries of both conformers and for the transition state (TS) between them were carried out using the closed-shell Hartree–Fock (HF) [78] and second- and fourth-order Møller–Plesset [79] perturbation (MPX, X = 2 and 4) methods. The effect on the predicted properties of the nitrous acid conformers, of carrying out MPX-FU (full; all electrons included in the excitations) instead of MPX-FC (frozen core; no excitations from the 1s orbitals on the heavy atoms) may or may not be important. It will be discussed in the appropriate sections. Complete geometry optimizations for both conformers and for the TS between them were also performed with density functionals (Becke's three parameter non-local exchange functional (B3LYP) [80, 81] with the non-local correlation functional of Lee *et al.* [82]) and with several basis sets including diffuse functions. (In tables 4–9 the notation + in the basis set description indicates extra s and p functions on the heavy atoms; ++ indicates the same plus extra s functions on the hydrogen atoms.) The relative energies of the conformers were determined by Gaussian 2 (G2) [83] calculations for comparison with the other results.

All computations were performed with the GAUSSIAN 94 program package [84], using standard basis sets, and the tight option for the optimizations. Some of the optimized geometrical parameters and the dipole moments μ (in debyes) are presented in tables 4, 5 and 6 (for *t*-HONO, for *c*-HONO and for the TS between them respectively). The rotational constants for the ground states of the rotamers are listed in table 7.

Harmonic fundamental vibrational frequencies were calculated for both conformers and the TS at most levels of theory used. The theoretical vibrational frequencies for the *t*-HONO and *c*-HONO conformers are listed in tables 8 and 9 respectively. The zero-point energies (ZPEs) are given in tables 4–6.

3. Results and discussion

The *t*- and *c*-HONO dipole moments, obtained by laser Stark spectroscopy, are μ = 1.930(17) D and μ = 1.428(7) D respectively [51]. An earlier microwave spectroscopy study yielded values of μ = 1.855(16) D and μ = 1.423(5) D for the *t*-^{15}N and *c*-^{15}N isotopomers respectively [53]. The difference between the two values for *t*-HONO is larger than the combined error limits; its origin has been discussed in [51].

It can be seen from tables 4 and 5 that both dipole moments are overestimated at almost all theoretical levels used in this work. The closest theoretical value for *t*-HONO is 2.06 D (B3LYP/6-311G** (table 4)). For *c*-HONO, the MP4SDTQ-FC/6-31G** value is 1.422 D (table 5) which is within experimental error of the above value.

Table 6. Predicted properties of the TS between the *t*- and *c*-HONO conformers: bond lengths, bond angles, barrier position ZPE of the optimized structures; energy difference between the *t*-HONO minimum and the TS; torsional barrier corrected for the ZPEs.

Method/basis	r(H–O) (Å)	r(O–N) (Å)	r(N=O) (Å)	∠(H–O–N) (degrees)	∠(O–N=O) (degrees)	θ (degrees)	ZPE(TS) (kJ mol^{-1})	ΔE (kJ mol^{-1})	Barrier (kJ mol^{-1})	References
HF/4-31G	0.9602	1.4497	1.1631	110.67	111.86	85.43	51.3	40.5	35.2	[60, 62, 64][a]
HF/6-31G	0.9592	1.4354	1.1680	111.47	112.06	85.40	51.7	42.3	36.7	[62, 64][a]
HF/6-311 +G**	0.9477	1.3871	1.1389	107.38	112.25	86.89	55.1	47.0	41.6	[62][a]
HF/6-311 ++G**	0.9477	1.3871	1.1389	107.37	112.25	86.90	55.1	47.1	41.7	[62][a]
B3LYP/6-311 ++G**	0.9704	1.5069	1.1552	104.96	111.67	86.48	47.3	53.9	48.3	[a]
MP2-FU/6-31 ++G**	0.9749	1.5257	1.1805	103.04	111.07	86.29	46.0	51.8	45.6	[a]
MP2-FU/6-311G**	0.9661	1.4947	1.1690	101.57	111.31	86.70	47.4	52.0	45.9	[a]
MP2-FU/6-311 +G**	0.9690	1.5119	1.1652	102.57	111.43	85.50	46.5	52.1	45.9	[a]
MP2-FC/6-311 ++G**	0.9695	1.5161	1.1655	102.46	111.40	85.50	46.4	51.9	45.6	[a]
MP2-FU/6-311 ++G**	0.9690	1.5120	1.1652	102.54	111.43	85.53	46.5	52.2	45.9	[a]

[a] This work.

Table 7. Rotational constants for the nitrous acid conformers.[a]

	t-HONO			*c*-HONO		
Method/basis	*A* (cm^{-1})	*B* (cm^{-1})	*C* (cm^{-1})	*A* (cm^{-1})	*B* (cm^{-1})	*C* (cm^{-1})
HF/4-31G**	3.40951	0.45154	0.39873	2.99174	0.47294	0.40838
HF/6-31G	3.29995	0.42821	0.37903	2.87626	0.44588	0.38604
HF/6-31G*	3.40178	0.45104	0.39824	2.98200	0.47211	0.40758
HF/6-31G**	3.40945	0.45455	0.39848	2.98738	0.47241	0.40790
HF/6-31 ++G**	3.44494	0.45045	0.39836	2.99843	0.47133	0.40730
HF/6-311G**	3.47024	0.45365	0.40120	3.03183	0.47500	0.41066
HF/6-311 ++G**	3.48971	0.45302	0.40097	3.03588	0.47395	0.40995
HF/6-31 +G(3df,2p)	3.47897	0.45345	0.40117	3.03571	0.47381	0.40984
B3LYP/6-31G**	3.08509	0.41907	0.36895	2.77903	0.44294	0.38205
B3LYP/6-311G**	3.13789	0.41852	0.36927	2.82861	0.44267	0.38277
B3LYP/6-311 ++G**	3.15320	0.41806	0.36912	2.83308	0.44055	0.38127
MP2-FU/4-31G**	3.02670	0.41762	0.36699	2.72588	0.44138	0.37987
MP2-FU/6-31G*	3.01671	0.41692	0.36630	2.71128	0.44000	0.37856
MP2-FU/6-31G**	3.02009	0.41703	0.36643	2.71883	0.44026	0.37890
MP2-FU/6-31 ++G**	3.03312	0.41399	0.36427	2.72504	0.43623	0.37603
MP2-FU/6-311G**	3.12658	0.42256	0.37225	2.79985	0.44675	0.38527
MP2-FU/6-311 +G**	3.12950	0.42037	0.37059	2.80097	0.44324	0.38268
MP2-FU/6-311 ++G**	3.12972	0.42039	0.37061	2.80186	0.44328	0.38273
MP4SDTQ-FC/6-31G**	2.96847	0.40771	0.35847	2.67851	0.43153	0.37165
MP4SDTQ-FC/6-311 +G**	3.05177	0.40850	0.36027	2.74871	0.43203	0.37335
Experimental[b]	3.098 544 08(37)	0.417 788 089(43)	0.367 476 383(40)	—	—	—
Experimental[c]	—	—	—	2.805 335 84(26)	0.439 273 149(44)	0.379 067 802(44)

[a] This work. [b] From [42] (Watson's *A* reduced Hamiltonian in the I^r representation). [c] From [60] (Watson's *A* reduced Hamiltonian in the I^r representation).

Table 8. Theoretical data (mode (symmetry species), approximate description) for the harmonic fundamental vibrational frequencies for *t*-HONO obtained for geometries optimized at the same theoretical level.[a] For the HF computations the IR intensities, Raman scattering activities A^4 and Raman depolarization ratios are given in parentheses. For the MP2 and BL3YP computations only the IR intensities are given.

Method/basis set	ν_1(a′) O−H stretch (cm^{-1}) (km mol^{-1}; amu; —) or (km mol^{-1}))	ν_2(a′) N=O stretch (cm^{-1}) (km mol^{-1}; amu; —) or (km mol^{-1}))	ν_3(a′) N−O−H bend (cm^{-1}) (km mol^{-1}; amu; —) or (km mol^{-1}))	ν_4(a′) N−O−H bend (cm^{-1}) (km mol^{-1}; amu; —) or (km mol^{-1}))	ν_5(a′) O=N−O bend (cm^{-1}) (km mol^{-1}; amu; —) or (km mol^{-1}))	ν_6(a″) N−O torsion (cm^{-1}) (km mol^{-1}; amu; —) or (km mol^{-1}))
HF/4-31G[b]	3988	1890.5	1415.3	900.7	721.9	552.8
HF/6-31G	4018 (133; 78; 033)	1902 (128; 16; 0.32)	1424 (219; 5; 0.75)	940 (211; 16; 0.28)	734 (30; 5; 0.43)	563 (206; 3; 0.75)
HF/6-31G*	4082 (125; 65; 0.31)	2043 (152; 26; 0.27)	1514 (263; 4; 0.73)	1098 (226; 9; 0.26)	790 (20; 2; 0.43)	599 (137; 2, 0.75)
HF/6-31G**	4148 (128; 65; 0.30)	2040 (155; 14; 0.27)	1496 (264; 4; 0.73)	1101 (224; 9; 0.26)	792 (19; 2; 0.44)	594 (136; 2; 0.75)
HF/6-311G**	4146 (135; 53; 0.33)	2040 (171; 13; 0.32)	1498 (263; 4; 0.75)	1088 (235; 9; 0.27)	800 (23; 3; 0.42)	588 (131; 2; 0.75)
HF/6-311 +G**	4135 (146; 59; 0.25)	2028 (191; 13; 0.36)	1495 (261; 4; 0.70)	1079 (255; 10; 0.33)	801 (23; 3; 0.31)	583 (138; 0; 0.75)
HF/6-311 ++G**	4135 (146; 59; 0.25)	2028 (191; 13; 0.36)	1495 (262; 4; 0.70)	1079 (255; 10; 0.33)	801 (24; 3; 0.31)	583 (139; 0; 0.75)
HF/6-31 +G(3df,2p)	4133 (139; 57; 0.21)	2013 (172; 12; 0.28)	1500 (254; 2; 0.46)	1085 (247; 9; 0.30)	798 (21; 3; 0.23)	597 (122; 0; 0.75)
B3LYP/6-31G**	3755 (57)	1792 (135)	1306 (188)	862 (144)	631 (83)	595 (106)
B3LYP/6-311G**	3774 (70)	1794 (163)	1297 (188)	834 (127)	619 (116)	589 (105)
B3LYP/6-311 ++G**	3762 (83)	1786 (195)	1291 (187)	812 (135)	614 (153)	581 (116)
MP2-FU/6-31G**	3814 (74)	1662 (68)	1304 (192)	865 (185)	630 (101)	601 (114)
MP2-FU/6-31 ++G**	3784 (90)	1656 (104)	1289 (189)	814 (187)	608 (168)	583 (122)
MP2-FC/6-311G**	3841 (87)	1687 (84)	1308 (192)	863 (178)	637 (125)	588 (107)
MP2-FU/6-311G**	3846 (88)	1691 (84)	1310 (192)	866 (179)	640 (124)	590 (108)
MP2-FU/6-311 +G**	3814 (97)	1683 (111)	1299 (189)	826 (176)	623 (182)	573 (116)
MP2-FC/6-311 ++G**	3810 (95)	1679 (111)	1296 (190)	823 (175)	620 (185)	571 (117)
MP2-FU/6-311 ++G**	3814 (97)	1683 (111)	1299 (190)	826 (177)	623 (183)	573 (117)
MP4SDTQ-FC/6-31G**	3796	1640	1280	817	580	594
MP4SDTQ-FC/6-311 +G**	3775	1650	1266	774	548	559

[a] All data, except for the HF/4-31G values, are from this work. [b] From [60].

Table 9. Theoretical data (mode (symmetry species), approximate description) for the harmonic fundamental vibrational frequencies for *c*-HONO obtained for geometries optimized at the same theoretical level.[a] For the HF computations the IR intensities, Raman scattering activities A^4 and Raman depolarization ratios are given in parentheses. For the MP2 and BL3YP computations only the IR intensities are given.

Method/basis set	ν_1(a′) O–H stretch (cm^{-1}) (km mol^{-1}; amu; —) or (km mol^{-1}))	ν_2(a′) N=O stretch (cm^{-1}) (km mol^{-1}; amu; —) or (km mol^{-1}))	ν_3(a′) N–O–H bend (cm^{-1}) (km mol^{-1}; amu; —) or (km mol^{-1}))	ν_4(a′) N–O–H bend (cm^{-1}) (km mol^{-1}; amu; —) or (km mol^{-1}))	ν_5(a′) O=N–O bend (cm^{-1}) (km mol^{-1}; amu; —) or (km mol^{-1}))	ν_6(a″) N–O torsion (cm^{-1}) (km mol^{-1}; amu; —) or (km mol^{-1}))
HF/4-31G[b]	3819	1826	1458	954	703	670
HF/6-31G	3847 (59; 73; 0.32)	1831 (190; 17; 0.36)	1467 (3; 7; 0.73)	998 (332; 6; 0.25)	710 (16; 8; 0.50)	675 (231; 4; 0.75)
HF/6-31G*	3939 (64; 53; 0.30)	1988 (232; 11; 0.30)	1542 (10; 4; 0.74)	1161 (343; 2; 0.20)	784 (16; 5; 0.47)	746 (152; 2; 0.75)
HF/6-31G**	4009 (64; 52; 0.29)	1986 (232; 11; 0.30)	1524 (11; 4; 0.74)	1166 (346; 2; 0.20)	784 (16; 5; 0.47)	742 (151; 2; 0.75)
HF/6-311G**	3998 (61; 51; 0.31)	1984 (240; 11; 0.38)	1522 (12; 5; 0.73)	1154 (365; 2; 0.21)	791 (17; 6; 0.46)	727 (148; 2; 0.75)
HF/6-311 ++G**	3991 (71; 56; 0.23)	1972 (267; 12; 0.36)	1512 (10; 4; 0.74)	1143 (398; 3; 0.31)	788 (15; 5; 0.35)	704 (153; 1; 0.75)
HF/6-31 +G(3df,2p)	3988 (68; 52; 0.18)	1959 (247; 12; 0.26)	1520 (11; 2; 0.74)	1147 (371; 3; 0.30)	787 (11; 5; 0.26)	712 (127; 1; 0.75)
B3LYP/6-31G**	3576 (15)	1726 (171)	1349 (6)	921 (265)	648 (15)	736 (109)
B3LYP/6-311G**	3583 (16)	1721 (187)	1338 (8)	893 (272)	638 (28)	718 (110)
B3LYP/6-311 ++G**	3583 (26)	1714 (222)	1322 (6)	871 (319)	626 (40)	684 (120)
MP2-FU/6-31G**	3645 (28)	1622 (118)	1348 (5)	948 (326)	655 (13)	746 (117)
MP2-FC/6-311G**	3656 (26)	1639 (123)	1338 (8)	945 (336)	665 (21)	722 (110)
MP2-FU/6-311G**	3659 (26)	1643 (124)	1341 (8)	948 (336)	667 (21)	724 (111)
MP2-FC/6-311 ++G**	3640 (36)	1630 (148)	1319 (7)	909 (390)	645 (35)	675 (120)
MP2-FU/6-311 ++G**	3642 (36)	1634 (148)	1321 (7)	912 (390)	648 (33)	678 (120)
MP4SDTQ-FC/6-31G**	3640	1578	1320	891	614	731
MP4SDTQ-FC/6-311 +G**	3617	1579	1290	851	589	657

[a] All data, except for the HF/4-31G values, are from this work. [b] From [60].

3.1. *Structural parameters*

The structural parameters of *t*-HONO are significantly different from those of *c*-HONO (see tables 3–5). This is believed to reflect the competitive interplay in *c*-HONO between the repulsive steric hindrance of the terminal atoms and the attractive hydrogen bonding between these same atoms; according to the best experimental determinations of the structure [54], they are separated by only 2.1 Å which is much less than the sum of the van der Waals radii for oxygen and hydrogen (2.6 Å).

It is interesting to note that, in contrast with the behaviour of the two terminal bonds, which are longer in *c*-HONO than in *t*-HONO, the central formal single O–N bond is shorter in *c*-HONO than in *t*-HONO (table 3).

3.1.1. *Experiment*

The first experimental determination of the structural parameters of *t*-HONO and *c*-HONO was reported by Jones *et al.* [7] in 1951. They gave identical values with each of the corresponding bond lengths in the two conformers. Except for *r*(O–N) for *c*-HONO, these bond lengths are within 0.03 Å of the best experimental values now available (see table 3). However, their estimation that the H–O–N and O–N=O bond angles were smaller by a few degrees in *c*-HONO than in *t*-HONO was later proven to be erroneous.

Substitution structures (r_s) for both conformers (table 3) were first reported by Cox *et al.* [53] who studied the microwave spectra of eight nitrous acid isotopomers. Small inertial defects, compatible with planar molecular structures, were determined for both conformers [53].

Equilibrium structural parameters r_e which should be used for comparison with theoretically optimized parameters, have been determined only for *t*-HONO (see table 3 and [52]). Using the observed fundamentals, their isotopic shifts and the centrifugal distortion constants (derived by analysing the centrifugal distortion shifts in the microwave spectra of *t*-HONO and *c*-HONO and their deuterated isotopomers), Finnigan *et al.* [52] determined 11 of the 16 force constants for each conformer. Use of this force field to evaluate the average moments of inertia led to the average structural parameters $\langle r \rangle$ given in table 3. Finnigan *et al.* [52] pointed out that the $\langle r \rangle$ are well defined structural parameters, only differing from the r_e because of the anharmonicity of the molecular vibrations. They also reported that, allowing for centrifugal distortion and electronic corrections, the inertial defects vanish for the average structures, showing conclusively that *t*-HONO and *c*-HONO are '*planar in the hypothetical average* (ground-vibrational) *state*' [52]. This finding has been confirmed in [54].

The most recent values for the zero-point-average structures (r_z in table 3) were calculated using microwave data for five isotopomers of *t*-HONO and three isotopomers of *c*-HONO and explicit isotopic shrinkage corrections [54]. The differences between these geometrical parameters and those reported earlier in [52] are attributed mainly to the isotopic shrinkage corrections [54].

3.1.2. *Theory*

The predicted variations of the optimized *ab initio* structural parameters on going from the *t*- to the *c*-HONO conformations are in good general agreement with the experimental data. Both the H–O–N and O–N=O bond angles are predicted to be larger by a few degrees in *c*-HONO than in *t*-HONO at all levels of theory investigated (see tables 4 and 5). This presumably indicates that the steric hindrance between the

terminal atoms in *c*-HONO is more important than the effect of intramolecular hydrogen bonding. However, the difference in the effects is not large enough to cause the conformer to be nonplanar. Indeed, all optimizations started from non-planar *gauche* geometries in this work (up to 60° from the *c*-HONO structure), using tight optimization criteria, went to completely planar *c*-HONO structures. Some relaxation of the *c*-HONO structure is brought about by a perceptible lengthening of both the formal single H–O and double N=O bonds, in comparison to the corresponding bonds in *t*-HONO (see tables 3–5). The central formal single O–N bond is predicted to be shorter in *c*-HONO, again in agreement with experiment. This structural behaviour is in sharp contrast with that predicted for 1,3-butadiene where the central C–C bond is predicted to be longer in the *gauche* than in the *s-trans* conformer and the formal double bond lengths are predicted to remain essentially constant [85]. For 1,3-butadiene, except for optimizations with a minimal basis set, the planar *s-cis* structure is predicted to be a TS between two equivalent *gauche* minima [85]. This is presumably because decreased steric hindrance in the *gauche* conformer is more important than increased resonance in the planar *s-cis* structure [85]. Note that, recently, experimental IR evidence in favour of the *gauche* conformation of 1,3-butadiene in the gas phase has been reported [86].

The HF optimized parameters give the largest average deviations from the experimental data: 2.1–2.7% from the r_e parameters for *t*-HONO and 2.7–3.3% from the $\langle r \rangle$ parameters for *c*-HONO. The largest individual differences between the experimental and theoretical parameters are found again for the HF optimized parameters, notably for *r*(O–N) and for the H–O–N bond angle. Comparison with the experimental parameters in table 3 shows that all the HF optimizations reported in tables 4 and 5 underestimate the internuclear distances and overestimate the H–O–N bond angle. In contrast, the experimental values of the O–N=O bond angle are reproduced satisfactorily for both conformers at all levels of theory reported. Also, all the MP optimized values of the H–O–N bond angles for both conformers are within 1° of the latest experimental data. It is interesting to note that, for nitric acid, Lee and Rice [87] found that MP2 optimizations at the double-zeta plus polarization (DZP) and triple zeta-plus double-polarization (TZ2P) level also gave very satisfactory values for the HON bond angle (102.1° and 102.0° respectively; experimental value, 102.15° [88]). Finally, note that the B3LYP/6-311 ++G** results for nitrous acid are as satisfactory as those obtained with the more costly MP4SDTQ-FC/6-311 +G** optimizations.

The major difference between the theoretical geometries of the planar conformers and the TS is the long central O–N bond in the latter. The predicted elongation of this bond on torsion away from the planar structures has been reported previously [60, 62, 68] and it is probably the result of reduced conjugation in the TS. However, by comparison with the other MP results in tables 4–6, it is apparent that the exceptional elongation of the bond obtained in the MP2-FU/4-31G optimization performed by Murto *et al.* [62] is partly due to the basis set and not to the MP2 method.

3.2. *Relative energies*

3.2.1. *Experiment*

The experimental determinations of the energy difference between the *c*- and *t*-HONO conformers, denoted by $\Delta E = E_{cis} - E_{trans}$, range from +1.56 to +2.70 kJ mol^{-1}, always in favour of *t*-HONO as the lowest-energy species [7, 49, 57, 58].

Jones *et al.* [7] determined $\Delta E = +2.12 \pm 0.11$ kJ mol^{-1} from the dependence, between 0 and 70 °C, of the intensities of the pairs of IR bands, 856 and 794 cm^{-1} (ν_4; O−N stretch) and 637 and 543 cm^{-1} (ν_6; O−N torsion) [7]. McGraw *et al.* [49] studied the intensities of the same IR bands (which they placed at 853, 791, 638 and 540 cm^{-1} respectively) between 0 and 46 °C and reported that $\Delta E = +2.22$ kJ mol^{-1}, quite close to the above value. However, they placed a much larger error bar (± 4 kJ mol^{-1}) on their determination [49]. This error bar, which seems to be extraordinarily large, would allow either conformer to be the lowest-energy one. More recently, Varma and Curl [57] determined the relative intensities of rotational transitions at room temperature and reported that $\Delta E = +1.56 \pm 0.17$ kJ mol^{-1} and $\Delta E = +2.04 \pm 0.15$ kJ mol^{-1} for the HONO and DONO conformers respectively. They suggested combining these results to yield an average value: $\Delta E = +1.69 \pm 0.42$ kJ mol^{-1} for HONO. Based on the assumption that the oscillator strength of the $\pi^* \leftarrow$ n transition of the two rotamers is the same, Bongartz *et al.* [58] determined the ratio $K = p_{trans}/p_{cis} = 3.25 \pm 0.30$ at 277 K. This ratio corresponds to $\Delta E = +2.70 \pm 0.21$ kJ mol^{-1}. They pointed out that this is probably accidentally nearly identical with 'recent theoretical results' [63] (and which, ironically, repeated the earliest theoretical result for complete geometry optimization of the HONO conformers with the same 4-31G basis set [60]). Compared with the ΔE determined by Varma and Curl [57], the value obtained by Bongarts *et al.* [58] appears to be rather high, although it could lie within the combined experimental uncertainties.

The relative energy of the conformers obtained in the microwave intensity measurements by Varma and Curl [57] must be considered to be the best to date. Nevertheless, considering the recent developments in the measurement of absolute intensities of IR absorption bands, it would be very interesting to have new experimental studies, similar to those of Jones *et al.* [7] and McGraw *et al.* [49], of which the latest was performed just over 30 years ago. Alternatively, perhaps use of the method of preparing nitrous acid at known concentrations from the reaction of gaseous HCl with solid sodium nitrite [28, 29] could be adapted to the determination of the relative conformer populations.

3.2.2. *Theory*

For molecules exhibiting rotational isomerism, it is well known that the theoretical relative energies of the conformers can depend strongly both on the structural parameters (bond lengths and angles, dihedral angles) and on the theoretical method used.

To obtain the heat ΔH of formation of a conformer, the ZPE must be added to the energy which is computed for an isolated molecule at 0 K. The theoretical values of the ZPE varies from 52.1 to 60.8 kJ mol^{-1} for *t*-HONO (table 4) and from 52.5 to 61.1 kJ mol^{-1} for *c*-HONO (table 5). However, for a given basis set or method the difference between the ZPEs for the two conformers is $|0.5|$ kJ mol^{-1} or less. Note also that the experimental ZPEs are equal for the two conformers, although the uncertainty in the frequencies of ν_3 and ν_5 of *c*-HONO must be taken into account.

The confusion arising from the many contradictory theoretical results on the relative energies of the nitrous acid conformers is exemplified by comparison of the experimental ΔE with those obtained from G1 and G2 computations (+3.17 and +2.33 kJ mol^{-1} respectively (this work)) and with the difference in their heats of formation obtained with the bond-additivity-corrected (BAC)-MP4 technique ($\Delta H = -5.9$ kJ mol^{-1} [74]). The BAC-MP4 results are thus in contradiction with

the experimental data in this case (see above) whereas the method has been shown to give reliable data for many other compounds with hydrogen, nitrogen and oxygen atoms [89].

3.2.2.1. *Hartree–Fock computations.* The most comprehensive early theoretical study on the effect of the basis set and theoretical level on the relative energies of the nitrous acid conformers is that by Murto *et al.* [62]. They reported 17 sets of computations, at different theoretical levels, with complete geometry optimization of the conformers. Only eight sets predicted *t*-HONO to be the lowest-energy conformer; the nine others placed *c*-HONO lower in energy than *t*-HONO. Using a larger basis set for the HF optimizations did not ensure better results [62].

The dependence of the calculated relative energies of the nitrous acid conformers on the molecular geometries used is clearly demonstrated by the literature results obtained with the minimal Slater-type orbital (STO)-3G basis set. Using the experimental geometries from [52], Benioff *et al.* [69] obtained $\Delta E = -11.2$ and -11.7 kJ mol^{-1} from HF/STO-3G and optimized valence configurations, configuration interaction (OVCCI)/STO-3G computations respectively. Complete geometry optimization of both conformers (HF/STO-3G//HF/STO-3G computations) inverts the relative energies ($\Delta E = +0.38$ kJ mol^{-1} [61–63, 65, 70]), bringing them into closer accord with experiment. Another, less marked example is found with the 4-31G basis set. In 1971, Radom *et al.* [71] used the 'standard geometries' of Pople and Gordon [72] to calculate the relative energies of the nitrous acid conformers and obtained fortuitously good agreement with the experimental data available at that time ($\Delta E = +1.88$ kJ mol^{-1}). However, HF/4-31G//HF/4-31G computations yield a higher value: $\Delta E = +2.68$ kJ mol^{-1} [60–63]. (The same value is obtained from the total energies given in table II of [65]; however, the relative energy given there ($\Delta E = +9.3$ kJ mol^{-1}) is incorrect.) The 'good' ΔE value obtained from the 4-31G optimizations of the HONO conformers is probably fortuitous. Indeed HF/3-21G optimizations yield a very different result: $\Delta E = -6.53$ kJ mol^{-1} [61, 62].

3.2.2.2. *Effect of including polarization and/or diffuse functions in the basis set.* Long-range interactions, especially intramolecular hydrogen bonding between the terminal atoms, are probably important in *c*-HONO [90–92]. Such interactions should be better accounted for at a theoretical level which includes polarization functions, diffuse functions, or both of these. However, note that Nguyen and Hegarty [61] and Murto *et al.* [62] found that adding polarization functions to a given basis set resulted in a *lowering* of the relative energy of *c*-HONO, bringing the results into further discord with experiment. For example, whereas HF/6-311G optimizations yield $\Delta E = +3.3$ kJ mol^{-1}, HF/6-311G** optimizations invert the relative energies to $\Delta E = -3.4$ kJ mol^{-1} [62].

Adding diffuse functions to a basis set lowers the relative energy of *t*-HONO [62, 65, 73]. From HF/6-311G**//HF/6-31G* single point computations, without diffuse functions, Turner [65] obtained $\Delta E = -3.5$ kJ mol^{-1}. In contrast, HF/6-311 ++G**//HF/6-31G* computations yielded $\Delta E = +0.5$ kJ mol^{-1} [65]. At about the same time, Murto *et al.* [62] reported that their 'best' near-HF-limit value, $\Delta E = +0.6$ kJ mol^{-1} (about 1 kJ mol^{-1} less than the best experimental value, see above) was obtained from HF/6-311 ++G** optimizations. The HF/6-311 ++G** ΔE given above is in partial disagreement with the reported findings of Coffin and Pulay [73] who state that 'addition of diffuse functions to the basis set (6-311G**) leads to

a stabilization of the *trans* form of the molecule, but not enough to lower it below the *cis* form'. We have therefore carried out HF/6-311 ++G**//HF/6-311 ++G** computations and confirmed the results of Murto *et al.* [62] (see table 5).

3.2.2.3. *Møller–Plesset perturbation theory*. A number of MP computations have been reported for nitrous acid (for examples see [22–24, 27, 62, 64–67, 73, 74]). Although the HF approximation is inadequate for this molecule, owing to strong electron correlation [73], using the MP method does not ensure better results. Indeed, the ΔE values obtained from MP computations only predict *t*-HONO to be the lowest-energy conformer when diffuse functions are included in the basis set (see table 5 and [62, 65, 73]). For example, Murto *et al.* [62] obtained $\Delta E = -5.29$ kJ mol^{-1} and $\Delta E = +7.025$ kJ mol^{-1} from MP2-FU optimizations with the 4-31G(N*) and 4-31 ++G(N*) basis sets respectively. (N* signifies polarization functions added only on the N atom.) Using HF/6-31G* optimized geometrical parameters for both conformers, Turner [65] carried out MP*X*-FU (*X* = 2, 3 and 4)/6-31G*, MP*X*-FU (*X* = 2, 3 and 4)/6-31G** and MP2-FU/6-31 ++G**//HF/6-31G* computations. He found that only the MP2-FU/6-311 ++G** computations predicted *t*-HONO to be the lowest-energy conformer ($\Delta E = +3.5$ kJ mol^{-1}). Recently, Coffin and Pulay [73] obtained $\Delta E = -0.505$ kJ mol^{-1} from MP4SDQ-FC/6-311G** optimizations and $\Delta E = +4.791$ kJ mol^{-1} from MP4SDQ-FC/6-311 ++G**//MP4SDQ-FC/6-311G** computations, emphasizing again the important effect of diffuse functions in the basis set on the relative energies of the conformers.

In a recent paper, Hsu *et al.* [74] reported optimized MP2-FC/6-311G** geometries which are identical within rounding off accuracy with the MP2-FC/6-311G** geometries that we published in 1995 [67]. Their energy difference for H + *c*-HONO and H + *t*-HONO is −0.6 kcal mol^{-1} (−2.5 kJ mol^{-1}) which is more negative than our value for the HONO conformers ($\Delta E = -1.79$ kJ mol^{-1} [67]). The difference may be due to the presence of the hydrogen-atom in their work. In table 1 of [27] there is an error in the MP2-FC/6-311G** energy reported for *c*-HONO (which should be −205.275261 hartree [67]). This erroneous energy was apparently used to obtain $\Delta E = -0.2$ kcal mol^{-1} [27] instead of −1.79 kJ mol^{-1} (see above).

Inclusion of the 1s orbitals on the heavy atoms in the substitutions (MP2-FU/6-311G** optimizations) lowers the total energy of each conformer by 0.055 hartree, leaving ΔE almost unchanged (−1.83 kJ mol^{-1} (this work) compared with the MP2-FC results.

The MP2-FU/6-311 +G**, MP2-FC/6-311 +G**, MP2-FU/6-311 +G** and MP4-FC/6-311 +G** optimizations all predict *t*-HONO to be the lowest-energy conformer, by nearly identical amounts. The results all lead to the conclusion that, to obtain the correct order for the relative energy of the nitrous oxide conformers from MP computations, the inclusion of diffuse functions is necessary. The ΔE values obtained are too large, however, being more than twice the most reliable experimental data.

3.2.2.4. *Density functionals.* As mentioned above, the best agreement between the theoretical and experimental geometrical parameters is obtained for the B3LYP optimized parameters at the three computational levels used in this work. Extending the basis set and, especially, including diffuse functions in the basis set have a very important incidence on the relative energies of the conformers; one obtains ΔE(B3LYP) = −3.76, −1.00 and +4.50 kJ mol^{-1} from the 6-31G**, 6-311G** and

6-311 ++G** optimizations respectively (table 5). (Mebel and co-workers [27, 74] reported ΔE(B3LYP/6-311G**) = − 0.2 kcal mol^{-1}, which is within rounding off error of our result.) Note that, although the relative energies obtained with the two sets of B3LYP optimizations without diffuse functions favour *c*-HONO as the lowest-energy conformer, they are closer to the experimental data (*t*-HONO lower in energy) than the corresponding MP2-FU results are (see table 5).

Whereas the B3LYP/6-311 ++G** optimizations yield a relative energy which is approximately twice the best experimental value, they correctly predict *t*-HONO to be the lowest-energy conformer.

3.2.2.5. *Configuration interaction; coupled clusters.* The first configuration interaction (CI) computations on both nitrous acid conformers and the TS between them were carried out by Benioff *et al.* [69] in 1976. Using 19 configurations, a double-zeta quality basis set and the optimized geometries reported by Skaarup and Boggs [68] they obtained ΔE = + 10.5 kJ mol^{-1} or about five to six times the experimental values (see above). From configuration interaction with double excitation (CID)/4-31G optimizations, including all orbitals in the excitations, Murto *et al.* [62] obtained a slightly lower value: ΔE = + 7.15 kJ mol^{-1}.

In recent work, [27, 75, 76], the absolute values reported for ΔE are much smaller but the results are contradictory; depending on the method used, either *c*-HONO or *t*-HONO is predicted to be the lowest-energy conformer. For instance, from single reference configuration interaction with single and double excitations (CISD) and coupled-electron-pair-approach (CEPA)-1 computations, Suter and Huber [75] obtained ΔE = − 0.72 kJ mol^{-1} and +0.36 kJ mol^{-1}, respectively. Lee and Rendell [76] used a triple zeta plus double polarization quality basis set to perform coupled clusters with single and double excitations (CCSD) and coupled clusters with single and double excitations with perturbative triples (CCSD(T)) optimizations on both conformers. Even with such a large basis set, the ΔE obtained are not very satisfactory: ΔE(CCSD) = − 0.14 kJ mol^{-1} and ΔE(CCSD(T)) = + 0.29 kJ mol^{-1} [76]. In their recent paper Mebel *et al.* [27] reported that CCSD(T)/6-311G(d, p) and QCISD(T)/6-311G(d, p) optimizations yield ΔE = − 0.3 and −0.2 kcal mol^{-1} respectively, again in discord with experiment.

3.3. *Rotational barrier*

3.3.1. *Experiment*

Using their experimental data and a three-term torsional potential function, Jones *et al.* [7] estimated the *t*-→ *c*-HONO and *c*-→ *t*-HONO barriers in the gas phase to be 50.2 and 48.1 kJ mol^{-1} respectively. They predicted the top of the barrier to be at about 88° from the *trans* minimum (θ = 92° where θ is the H−O−N=O dihedral angle; θ = 0° and 180° for *c*- and *t*-HONO respectively). McGraw *et al.* [49] used a three-term torsional potential and estimated the *t*-→ *c*-HONO and *c*-→ *t*-HONO barriers in the gas phase to be 48.4 ± 0.8 and 43.0 ± 0.8 kJ mol^{-1} respectively. Although these values are close to the results of Jones *et al.* [7], they yield a higher energy difference between the rotamers. McGraw *et al.* [49] placed the barrier maximum at θ = 86°, very close to later theoretical predictions (see below).

Kinetic studies of the *in-situ* IR photoinduced isomerization of HONO, which was produced by UV photolysis of HN_3 and O_2 mixtures in nitrogen or argon matrices, has permitted the determination of the upper limits to the torsional barriers in those environments [12–15]. Hall and Pimentel [12] reported that both *c*-→ *t*-HONO and

t-→ *c*-HONO processes occurred. During unfiltered IR photoinduced isomerization experiments, the intensities of the IR bands attributed to ν_4 of *t*-HONO (or *t*-DONO) increased, with a concurrent decrease in the intensities of the ν_4 bands of *c*-HONO (or *c*-DONO) (see figure 3 in [12]). The effective range for the IR photoinduced isomerization was 3200–3650 cm^{-1}, corresponding to 9.7 ± 0.7 kcal mol^{-1} (40.6 ± 2.9 kJ mol^{-1}) for the *t*-→ *c*-HONO torsional barrier height in the matrix at 20 K. The *c*-→ *t*-HONO barrier in the gas phase was estimated to be lower, 36.4 ± 4 kJ mol^{-1} [12]. Note that the phenomena influencing the rates of the IR photoinduced isomerization of nitrous acid in various low-temperature matrices has been studied theoretically using molecular mechanics. The authors of [77] maintain that the results of the calculations support a mechanism in which the energy is absorbed specifically into the O−H vibrational mode and then undergoes a vibration → lattice phonon modes → rotation → torsional vibration migration (see [77] and references cited therein).

From specific IR laser excitation into the ν_1 and $2\nu_2$ modes of each conformer, in both nitrogen and argon matrices, Shirk and coworkers [14, 15] showed that the photoisomerization is a single-photon process, even though the photoinduced rate of the *c*-→ *t*-HONO isomerization was always much faster than that of the corresponding *t*-→ *c*-HONO isomerization. This has been attributed to a stronger coupling between the torsional mode ν_6 and the ν_1 and ν_2 modes in *c*-HONO than in *t*-HONO [14, 15, 90]. Shirk and Shirk [15] determined the barrier height for the *c*-→ *t*-HONO torsion in the nitrogen matrix to be about equal to $2\nu_2$ of *c*-HONO or 3250 ± 100 cm^{-1} (38.9 ± 1.2 kJ mol^{-1}). Combining this value with $\Delta E = +1.69 \pm 0.42$ kJ mol^{-1} [57], one obtains 40.6 ± 1.7 kJ mol^{-1} for the *t*-→ *c*-HONO barrier. These values indicate that the earlier estimates [7, 49] are slightly too high.

3.3.2. *Theory*

The values of the theoretical barriers to the torsional motion depend on the relative energies of the potential minima and the TS between them, corrected by the differences in the ZPE (ΔZPE = ZPE(*t*-HONO)-ZPE(TS)). (The imaginary frequency obtained for the torsional mode in the TS is neglected.) ΔZPE is expected to be very close to 5 kJ mol^{-1} and accounting for it lowers the barrier by about 10–15% (see table 6). The theoretical ZPEs determined for *t*- and *c*-HONO, with a given basis set and method, are nearly identical (see section 3.2.2). The accuracy of the torsional barrier height will depend on how accurately the theoretical geometry represents that of the TS and on the validity of the corresponding wavefunction. The results of early work in which the TS structure was not optimized [69, 71, 77] will not be discussed in detail. Also, the data in table 6 are restricted to the theoretical methods which predicted the *t*-HONO conformer to be the lowest-energy one.

In the first study of the torsional potential in which complete relaxation of the molecular geometry was allowed, Skaarup and Boggs [68] used a double-zeta quality basis set and carried out geometry optimizations at the TS and nine fixed torsional angles. They found the TS to be at $\theta = 85.47°$, 36.4 kJ mol^{-1} above the *c*-HONO minimum (which, as noted above, was only 0.1 kJ mol^{-1} lower than the *trans* minimum in their work). Note that the torsional barrier was not corrected for ΔZPE.

In their comprehensive study of HONO at the HF/4-31G level of theory, Farnell and Ogilvie [60] reported the energies for optimizations at seven torsional angles. These included the *trans* and *cis* conformations and the TS for which they found $\theta =$ 1.492 rad (85.48°). This is remarkably and no doubt fortuitously close to the TS

position determined by Skaarup and Boggs [68] with the larger basis set. In HF/4-31G optimizations (tight criteria), we obtained $\theta = 85.43^\circ$ in excellent agreement with the work of Farnell and Ogilvie [60] and Murto *et al.* [62]. Note that the HF/4-31G computations yield 40.5 kJ mol^{-1} for the $t \rightarrow c$-HONO barrier, uncorrected for ΔZPE [60, 62, 63, 65], very close to the values deduced from the IR photoinduced isomerization experiments [12–15]. However, introducing the ΔZPE lowers this value to 35.2 kJ mol^{-1} (this work).

Turner [65] reported 15 values, ranging from 36 to 62 kJ mol^{-1}, for the torsional barrier in nitrous acid. These values were all uncorrected for ΔZPE and most of them were obtained for geometries optimized at a lower theoretical level.

For completely optimized geometries, Murto *et al.* [62] also reported the following values for the $t \rightarrow c$-HONO barrier (uncorrected for ΔZPE): 44.26 kJ mol^{-1} (HF/6-311G), 47.08 kJ mol^{-1} (HF/6-311 ++G**) ($\theta = 86.9^\circ$) and 41.2 kJ mol^{-1} (MP2/4-31G) ($\theta = 83.6^\circ$). These computational levels were chosen for optimization of the TS because they all predict *t*-HONO to be the lowest-energy conformer [62].

The TS between the conformers is predicted to be closer to the *c*-HONO minimum, with its position being remarkably constant; θ only varies from 85.40° to 86.90° (table 6). Comparison of the predicted barrier heights for the $t \rightarrow c$-HONO torsion (ΔE(TS)) with the best experimental determination (38.9 kJ mol^{-1} $\leqslant \Delta E$(TS) $\leqslant$ 42.3 kJ mol^{-1} [15]) shows that only the HF/6-311 +G** and HF/6-311 ++G** values fall within the experimental error limits. The ΔE(TS) obtained from all the HF computations without polarization and diffuse functions are too low. The value determined from the B3LYP computations is the highest, 14% above the upper experimental limit, whereas all the MP2 values are about 6% higher than the upper experimental limit.

3.4. *Rotational constants*

Experimental values for the rotational constants of the nitrous acid conformers have been determined with high accuracy [41, 42]. In theoretical computations the rotational constants calculated for the input and optimized geometries are routinely part of the output listings. Whereas the near coincidence between the experimental and theoretical rotational constants can be a decisive factor in the assignment of a fundamental vibrational band to a given rotational conformer [86], the theoretical constants are not usually reported in the literature. The agreement between the experimental and theoretical constants is also a measure of the agreement between the true and the optimized geometries. The rotational constants calculated for the optimized *t*- and *c*-HONO geometries are given in table 7 together with the latest experimental data for the ground vibrational state [42, 50].

The rotational constants calculated for the ground vibrational state of both nitrous acid conformers with the HF optimized geometries are all overestimated. This is especially true for the *A* constant for *t*-HONO where, except for the HF/4-31G and HF/6-31G values, the overestimations are from 10 to 13%.

In contrast, except for the results obtained with the 6-311G** basis set (with and without diffuse functions), the MP2 optimized geometries all lead to a small underestimation of the three rotational constants for *t*-HONO and of the *A* constant for *c*-HONO. The rotational constants calculated with the MP4 optimized geometries are also underestimated (from 1.5 to 4.5%). Nevertheless, more than half of the rotational constants calculated with the MP optimized geometries lie within 1% of the corresponding experimental value. The difference between the HF and MP results

with the same basis set is attributed mainly to the effect of relaxation of the molecular structure due to electron correlation in the MP computations.

The B3LYP/6-31G** optimized geometries yield constants that are the closest to the experimental values: within 0.4% and 0.8% for *t*-HONO and *c*-HONO respectively. The maximum deviation of the other B3LYP values is only 1.8%. This is in direct accord with the above observation that the B3LYP optimized geometrical parameters deviate the least from the experimental values (section 3.1.2).

3.5. *Vibrational frequencies*

3.5.1. *Experiment*

There are two recent compilations of the fundamental vibrational frequencies of the *t*-HONO and the *c*-HONO conformers [93, 94]. As mentioned in the introduction, all the fundamental vibrational frequencies of *t*-HONO in the gas phase are known to at least five significant figures (table 2). They will only be discussed where comparison with the frequency data for *c*-HONO makes this necessary. The small energy difference between the *t*- and *c*-HONO conformers makes it possible to observe IR bands for both of them and, by substitution of the hydrogen atom by deuterium, to distinguish easily which bands pertain to the ν_1 mode (O–H stretch) of both conformers and to the ν_3 mode (H–O–N bend) of *t*-HONO. In contrast, the ν_3 mode of *c*-HONO is predicted to have a very low IR intensity. The same is true for ν_5 (O=N–O bend) of *c*-HONO. Thus there have been only tentative assignments of experimentally observed bands to these two modes [4, 5, 7, 11, 16, 46, 48, 49]. They will be discussed in detail below.

Although all the fundamental modes of both conformers should be active in the Raman measurements, there are apparently no data available for the Raman spectra of nitrous acid [93, 94]. This is presumably due to the complexity of the gaseous mixtures (see the introduction).

3.5.1.1. *c-HONO: ν_3 (N–O–H bend), gas phase*. D'Or and Tarte [4, 5] assigned a pair of bands at about 1370 and 1267 cm^{-1}, which seemed to undergo concurrent decreases to 1086 and 1015 cm^{-1} upon deuteration, to the H–O–N and D–O–N bending modes of the respective *cis* and *trans* conformers. However, it is probable that the band they observed at about 1370 cm^{-1} was due to another molecular H, N, O species. Indeed, using a harmonic force field, Deeley and Mills [40] predicted that ν_3 = 1298.7 cm^{-1} for *c*-HONO. As we shall see below, frequency calculations using scaled quantum-mechanical force fields also predict the frequency of ν_3(*c*-HONO) to be less than 1300 cm^{-1} but higher than that of ν_3(*t*-HONO) [67]. Jones *et al.* [7] observed a weak maximum centred at about 1292 cm^{-1} which they tentatively assigned to ν_3(*c*-HONO) because the out-of-plane torsional frequency for *c*-HONO is higher than that of the *trans* conformer. This is a plausible frequency but other N, O-containing species exhibit absorption bands in this region (N_2O, *asym*-N_2O_3, etc. [41, 93]). Later, McGraw *et al.* [49] observed a weak band in the gas phase IR spectrum at 1261 cm^{-1} which they assigned to ν_3(*c*-HONO). They pointed out that N_2O_4 has a *PQR* fundamental centred at 1261 cm^{-1} (*Q* branch at 1261.10 cm^{-1} [95]) but they ruled it out on the basis of its intensity, relative to the intensities of other vibrational bands for the tetraoxide in the spectra. However, the strongest caveat against the assignment of this weak band to ν_3(*c*-HONO) is found in the higher-resolution work where all observed lines near 1261 cm^{-1} can be assigned to the strong ν_3 fundamental of *t*-HONO, centred at 1263.2 cm^{-1} in the gas phase (table 2) [41, 46].

In their FTIR study of HONO, Guilmot [41] and Guilmot *et al.* [42] assigned some 2800 a-type lines and 1000 b-type lines to the ν_3 band of *t*-HONO in the spectral region extending from 1180.9 to 1309.8 cm^{-1}. They found no evidence for ν_3(*c*-HONO). However, in a laser Stark spectroscopy study, Maki [48] reported that a number of transitions observed near 1223 cm^{-1} could not be assigned to the ν_3 fundamental of *t*-HONO. Maki proposed that they are probably due to the ν_3(*c*-HONO) and may be the weak B-type band whose *Q* branches are barely discernible in figure 4 of [55].

3.5.1.2. *c-HONO: ν_3(N–O–H bend), matrix results.* Matrix effects are known to enhance the intensities of certain IR bands. Thus the bands at 1259.4–1263.3 cm^{-1} [11] and the medium-intensity bands at 1265–1267 cm^{-1} [16] observed for samples in argon matrices were assigned to *c*-HONO and would therefore correspond to its ν_3 fundamental mode. (The doubling of the frequencies is attributed to the occupation of different matrix sites by the monomer.) However, there are no other bands which can be assigned to the much stronger ν_3 fundamental of *t*-HONO in the spectra (see figure 1 of [11] and table 1 of [16]). These bands are thus most probably due to *t*-HONO and, as in [23, 24], show that ν_3(*t*-HONO) does not undergo an important frequency shift in an argon matrix. This is in sharp contrast with its behaviour in a nitrogen matrix where it is shifted by about +30 cm^{-1} (i.e. to 1293.7 cm^{-1} [9] or 1298 cm^{-1} [12]). (Chen *et al.* [10] have reported similar behaviour for the H–O–N bending frequency of nitric acid (+1.6 and +43.6 cm^{-1} in argon and nitrogen matrices respectively).) It is important to note here that theoretical calculations, with both scaled and unscaled quantum-mechanical force fields, place ν_3(*c*-HONO) at a frequency higher than that of ν_3(*t*-HONO) (see tables 7 and 8 in [67] and tables 8 and 9 in this work).

3.5.1.3. *c-HONO: ν_5 (O=N–O bend).* McGraw *et al.* [49] assigned a weak band at 608 cm^{-1} in the gas-phase spectrum to this fundamental. Although Deeley and Mills [46] made a tentative assignment of a band at 609.0 cm^{-1} to ν_5, they placed a caveat on the assignment; the poor signal-to-noise ratio of the FTIR spectrum in this region prevented a rotational analysis of the band. Later, Deeley *et al.* [45] investigated this spectral region at higher resolution and concluded that the lines belong to the *R* branch of ν_5(*t*-HONO). They conclude further that ν_5(*c*-HONO) has probably never been observed but that it lies close to ν_6(*c*-HONO) and is the cause of perturbations to the latter.

For nitrous acid in argon matrices, bands at 608.0–605.1 cm^{-1} [11] and 610 cm^{-1} [16] have been attributed to the ν_5(*c*-HONO). These values place the O–N–O bend frequency below that for the torsion about the central N–O bond and disagree with the value, 721 cm^{-1}, assigned to it for annealed nitrous acid at −190 °C [49]. This latter value seems to be anomalously high and, as we shall see below, disagrees with results obtained with scaled quantum-mechanical force fields.

3.5.2. *Theory*

There have been a large number of calculations of the theoretical harmonic frequencies for nitrous acid using quantum-mechanical force fields (for examples see [22, 23, 27, 60, 62, 64, 67, 68, 73, 76]). The unscaled harmonic theoretical fundamental frequencies, calculated at the theoretical level used to optimize the geometries, are listed in tables 8 and 9.

3.5.2.1. *t-HONO.* Comparison of the data in table 8 with those in table 2 shows that, as is generally observed, all the frequencies calculated with the unscaled HF force fields

are overestimated. The overestimation is smallest for ν_6 (2–10%) and largest for the ν_3 and ν_4 modes (up to 39%). The B3LYP frequencies present the smallest overall deviations from the experimental data; whereas the MP frequencies are closer to the experimental data than the corresponding HF values, they all underestimate the frequency for the ν_2 fundamental. The calculations at the highest level used in this work, MP4SDTQ-FC/6-311 +G**, also underestimate the ν_4 (2%) and ν_5 (8%) modes. These underestimations have no physical meaning and indicate inadequacies in the MP wavefunctions [67].

3.5.2.2. *c-HONO.* The frequency calculations using the unscaled HF force fields all yield $\nu_5 > \nu_6$. The situation is reversed for all the frequency calculations using the B3LYP and MP force fields. This is in accord with the observation by Murto *et al.* [62] that MP2 and CID calculations gave the ν_5 and ν_6 frequencies of *c*-HONO in the reversed order, compared with the values obtained at the HF levels.

Note that transferring the scale factors obtained for the HF/6-311G** force field for *t*-HONO to the corresponding force field for *c*-HONO yields $\nu_5 = 590\ cm^{-1}$ and $\nu_6 = 673\ cm^{-1}$ [67]. This is a large difference and it is a good indication that ν_5 is indeed at a lower frequency than ν_6 for *c*-HONO.

3.5.3. *Infrared intensities of the fundamental bands*

Experimental values of the absolute intensities I of the vibrational fundamentals of nitrous acid are apparently only available for ν_1, ν_2, ν_3 and ν_4 of *t*-HONO and ν_1, ν_2 and ν_4 of *c*-HONO [41, 55]. From the results of Kagann and Maki [55], one obtains $I(\nu_1, t):I(\nu_2, t):I(\nu_3, t):I(\nu_4, t):I(\nu_1, c):I(\nu_2, c):I(\nu_4, c) = 0.24:0.60:0.70:0.79:0.13:0.82:1.0$. The most recent values, obtained from FTIR line intensity measurements of ν_3 and ν_4 of *t*-HONO and ν_4 of *c*-HONO [41], are about 40% lower than the previous values. However, the ratios of the intensities determined in the two studies are fairly close: $I(\nu_3, t):I(\nu_4, t):I(\nu_4, c) = 0.66:0.70:1.0$ [41] compared with $0.70:0.79:1.0$ [55]. Also both studies agree that, at equal conformer concentrations, ν_4 of *c*-HONO has the highest absolute intensity. (Note, however, that this result depends directly on the calculated conformer concentrations.)

Comparison of the data in tables 8 and 9 shows that the computed intensities depend on both the theoretical method and the basis set used. For instance the HF/6-311 ++G** calculations yield $I(\nu_1, t):I(\nu_2, t):I(\nu_3, t):I(\nu_4, t):I(\nu_1, c):I(\nu_2, c):I(\nu_4, c) = 0.37:0.48:0.66:0.64:0.18:0.67:1.0$, conserving the relative order of the experimental intensities for most of these bands.

For *c*-HONO, the calculated IR intensities of the ν_3 and ν_5 bands are indeed low: 3% or less and 12% or less respectively of the calculated intensity of ν_4, computed to be the strongest band.

There is a marked discord, however, for the relative intensity of ν_5 for *t*-HONO, computed at the HF level on the one hand and computed at the B3LYP and MP levels on the other hand. Curiously enough, this marked discrepancy is not observed for ν_5 of *c*-HONO. For all the computations reported in table 8, one finds that $I(\nu_3, t)$ is somewhat higher than $I(\nu_4, t)$ in apparent contradiction with the above experimental ratios.

4. Conclusions

All the geometrical parameters for the planar *t*- and *c*-HONO conformers have been determined with accuracies which permit critical comparison with the optimized theoretical parameters. It is noteworthy that the experimental values of the O–N=O

bond angle for both conformers are reproduced satisfactorily at all levels of theory. However, the HF optimizations reported in this work invariably underestimate the internuclear distances and overestimate the H–O–N bond angle. Moreover, the largest individual differences (for the central formal single O–N bond length and for the H–O–N bond angle respectively) and largest average deviations from the experimental data are observed for the HF optimized parameters. In contrast, the MP optimizations for both conformers all predict values of the H–O–N bond angles which are within 1° of the latest experimental data. Density functional theory (B3LYP) yields optimized geometrical parameters that are the closest to the experimental data.

Experimentally, *t*-HONO is found to be lower in energy than *c*-HONO. The best determination for nitrous acid in the gas phase is $\Delta E = +1.69 \pm 0.42$ kJ mol^{-1} [57]. The difficulty encountered in reproducing such a small energy difference in theoretical computations is exemplified by the results presented in this paper. In general, adding polarization functions to a given basis set, without diffuse functions, results in a lowering of the relative energy of *c*-HONO, bringing the results into further discord with the experimental data. In contrast, including diffuse functions in the basis set results in a lowering of the relative energy of the *t*-HONO conformer at all levels of theory studied (HF, B3LYP and MP).

The best experimental estimate for ΔE(TS) (barrier to the $t \rightarrow c$-HONO torsion) is 40.6 ± 1.7 kJ mol^{-1} (see section 3.3.1.). The theoretical optimizations predict the position of the top of the barrier to be closer to the *c*-HONO minimum: $\theta = 85.40 \pm 0.75°$ (table 6). The ΔE(TS) obtained from all the HF computations without polarization and diffuse functions are too low; only the HF/6-311 +G** and HF/6-311 ++G** values fall within the experimental error limits. The value determined from the B3LYP computations is the highest, 14% above the upper experimental limit whereas all the MP2 values are acceptable, being about 6% higher than the upper experimental limit.

For *t*-HONO the largest overestimations of the HF frequencies are observed for the ν_3 and ν_4 modes (up to 39%). The B3LYP frequencies present the smallest overall deviations from the experimental data; whereas the MP frequencies are closer to the experimental data than the corresponding HF values, they all underestimate the frequency of the ν_2 fundamental. The MP4SDTQ-FC/6-311 +G** also underestimate the ν_4 (2%) and ν_5 (8%) modes. These underestimations have no physical meaning and indicate inadequacies in the MP wavefunctions [67, 88].

All computations indicate that the frequency of ν_3(*c*-HONO) is higher than that for ν_3(*t*-HONO). It is thus highly probable that the former has not been observed and that assignments of bands near 1265 cm^{-1} to *c*-HONO in argon matrices are incorrect.

For *c*-HONO the frequencies calculated with the unscaled HF force fields all place $\nu_5 > \nu_6$ whereas the situation is reversed for all the B3LYP and MP frequencies. Transferring the scale factors obtained for the *t*-HONO conformer HF/6-311G** force field to the corresponding force field of *c*-HONO yields $\nu_5 = 590$ cm^{-1} and $\nu_6 = 673$ cm^{-1} [67], a very good indication that ν_5 is indeed at a lower frequency than ν_6 for *c*-HONO.

Acknowledgments

The authors thank Dr Yurii N. Panchenko (M.V. Lomonosov Moscow State University), Dr Jean Olbregts (Université Libre de Bruxelles) and Dr Jean Vander Auwera (Université Libre de Bruxelles) for many helpful discussions.

References

[1] KIRCHNER, J. J., SIGURDSSON, S. TH., and HOPKINS, P. B., 1992, *J. Am. Chem. Soc.*, **114**, 4021.
[2] MELVIN, E. H., and WULF, O. R., 1931, *Phys. Rev.*, **38**, 2294.
[3] MELVIN, E. H., and WULF, O. R., 1935, *J. chem. Phys.*, **3**, 755.
[4] D'OR, L., and TARTE, P., 1951, *Bull. Soc. R. Sci. Liège*, **20**, 478.
[5] D'OR, L., and TARTE, P., 1951, *J. chem. Phys.*, **19**, 1064.
[6] TARTE, P., 1950, *Bull. Soc. chim. Belges*, **59**, 365–376.
[7] JONES, L. H., BADGER, R. M., and MOORE, G. E., 1951, *J. chem. Phys.*, **19**, 1599.
[8] (a) NGUYEN, M. T., SUMATHI, R., SENGUPTA, D., and PEETERS, J., 1998, *Chem. Phys.*, **230**, 1; (b) WANG, X., and QIN, Q., 1997, *Wuli Huaxue Xuebao*, **13**, 308.
[9] KOCH, T. G., and SODEAU, J. R., 1995, *J. phys. Chem.*, **99**, 10824.
[10] CHEN, W.-J., LO, W.-J., CHENG, B.-M., and LEE, Y.-P., 1992, *J. chem. Phys.*, **97**, 7167.
[11] CROWLEY, J. N., and SODEAU, J. R., 1989, *J. phys. Chem.*, **93**, 4785.
[12] HALL, R. T., and PIMENTEL, G. C., 1963, *J. chem. Phys.*, **38**, 1889.
[13] BALDESCHWIELER, J. D., and PIMENTEL, G. C., 1960, *J. chem. Phys.*, **33**, 1008.
[14] SHIRK, A. E., and SHIRK, J. S., 1983, *Chem. Phys. Lett.*, **97**, 549.
[15] MCDONALD, P. A., and SHIRK, J. S., 1982, *J. chem. Phys.*, **77**, 2355.
[16] GUILLORY, W. A., and HUNTER, C. E., 1971, *J. chem. Phys.*, **54**, 598.
[17] BECKER, K. H., KLEFFMANN, J., KURTENBACH, R., and WIESEN, P., 1996, *J. phys. Chem.*, **100**, 14984.
[18] BECKER, K. H., KLEFFMANN, J., KURTENBACH, R., and WIESEN, P., 1997, *Transport and Transformation of Pollutants in the Troposphere*, Proceedings of the Eurotrac Symposium '96, Vol. 1, edited by P. M. Borrell, P. Borrell, T. Cvitaš, K. Kelly and W. Seiler (Southampton, UK: Computational Mechanics Publications), pp. 355–359.
[19] COX, R. A., and DERWENT, R. G., 1976, *J. Photochem.*, **6**, 23.
[20] WAHNER, A., and BECKER, D., 1997, *Transport and Transformation of Pollutants in the Troposphere*, Proceedings of the Eurotrac Symposium '96, Vol. 1, edited by P. M. Borrell, P. Borrell, T. Cvitaš, K. Kelly and W. Seiler (Southampton, UK: Computational Mechanics Publications), pp. 317–321.
[21] KLEFFMANN, J., BECKER, K. H., and WIESEN, P., 1997, *Paul Scherer Institute Proc.*, **97-02**, 32.
[22] PAGSBERG, P., RATAJCZAK, E., SILLESEN, A., and LATAJKA, Z., 1994, *Chem. Phys. Lett.*, **227**, 6.
[23] MIELKE, Z., TOKHADZE, K. G., LATAJKA, Z., and RATAJCZAK, E., 1996, *J. phys. Chem.*, **100**, 539.
[24] MIELKE, Z., LATAJKA, Z., KOLODZIEJ, J., and TOKHADZE, K. G., 1996, *J. phys. Chem.*, **100**, 11610.
[25] KRAJEWSKA, M., and MIELKE, Z., 1998, *Pol. J. Chem.*, **72**, 335.
[26] KAISER, E. W., and WU, C. H., 1977, *J. phys. Chem.*, **81**, 1701.
[27] MEBEL, A. M., LIN, M. C., and MELIUS, C. F., 1998, *J. phys. Chem.* A, **102**, 1803 and references therein.
[28] BECKER, K. H., KURTENBACH, R., WIESEN, P., FEBO, A., GHERADHI, M., and SPARAPANI, R., 1995, *Geophys. Res. Lett.*, **22**, 2485.
[29] FEBO, A., PERRINO, C., GHERALDHI, M., and SPARAPANI, R., 1995, *Environ. Sci. Technol.*, **29**, 2390.
[30] TSANG, W., and HERRON, J. T., 1991, *J. Phys. Chem. Ref. Data*, **20**, 609, and references therein.
[31] CALVERT, J. G., YARWOOD, G., and DUNKER, A. M., 1994, *Res. Chem. Intermed.*, **20**, 463.
[32] FENTER, F. F., and ROSSI, M. J., 1997, *Transport and Transformation of Pollutants in the Troposphere*, Proceedings of the Eurotrac Symposium '96, Vol. 1, edited by P. M. Borrell, P. Borrell, T. Cvitaš, K. Kelly and W. Seiler (Southampton, UK: Computational Mechanics Publications), pp. 309–315.
[33] COX, R. A., 1974, *J. Photochem.*, **3**, 175.
[34] LAMMEL, G., and CAPE, J. N., 1996, *Chem. Soc. Rev.*, **25**, 361.
[35] ANDRÉS-HERNANDEZ, M. D., NOTHOLT, J., HJORTH, J., and SCHREMS, O., 1996, *Atmos. Environ.*, **30**, 175.
[36] STAFFELBACH, T., and NEFTEL, A., 1997, *Transport and Transformation of Pollutants in the*

Troposphere, Proceedings of the Eurotrac Symposium '96, Vol. 1, edited by P. M. Borrell, P. Borrell, T. Cvitaš, K. Kelly and W. Seiler (Southampton, UK: Computational Mechanics Publications), pp. 905–910.
[37] Matsumoto, M., 1997, *Kankyo Gijutsu*, **26**, 826.
[38] Matsumoto, M., and Okita, T., 1998, *Atmos. Environ.* **32**, 1419.
[39] Holland, S. M., Strickland, R. J., Ashfold, M. N. R., Newnham, D. A., and Mills, I. M., 1991, *J. chem. Soc., Faraday Trans.*, **87**, 3461, and references therein.
[40] Deeley, C. M., and Mills, I. M., 1985, *Molec. Phys.*, **54**, 23.
[41] Guilmot, J.-M., DSc Thesis, Université Libre de Bruxelles, Brussels, March 1993 (in French).
[42] Guilmot, J. M., Godefroid, M., and Herman, M., 1993, *J. molec. Spectrosc.*, **160**, 387.
[43] Guilmot, J. M., Carleer, M., Godefroid, M., and Herman, M., 1990, *J. molec. Spectrosc.*, **143**, 81.
[44] Kleiner, I., Guilmot, J. M., Carleer, M., and Herman, M., 1991, *J. molec. Spectrosc.*, **149**, 341.
[45] Deeley, C. M., Mills, I. M., Halonen, L. O., and Kauppinen, J., 1985, *Can. J. Phys.*, **63**, 962.
[46] Deeley, C. M., and Mills, I. M., 1983, *J. molec. Struct.*, **100**, 199.
[47] Maki, A. G., and Sams, R. L., 1983, *J. molec. Struct.*, **100**, 215.
[48] Maki, A. G., 1988, *J. molec. Spectrosc.*, **127**, 104.
[49] McGraw, G. E., Bernitt, D. L., and Hisatsune, I. C., 1966, *J. chem. Phys.*, **45**, 1392.
[50] Guilmot, J. M., Mélen, F., and Herman, M., 1993, *J. molec. Spectrosc.*, **160**, 401.
[51] Allegrini, M., Johns, J. W. C., McKellar, A. R. W., and Pinson, P., 1980, *J. molec. Spectrosc.*, **80**, 446.
[52] Finnigan, D. J., Cox, A. P., Brittain, A. H., and Smith, J. G., 1972, *J. chem. Soc., Faraday Trans. II*, **68**, 548.
[53] Cox, A. P., Brittain, A. H., and Finnigan, D. J., 1971, *J. chem. Soc., Faraday Trans.*, **67**, 2179.
[54] Cox, A. P., Ellis, M. C., Attfield, C. J., and Ferris, A. C., 1994, *J. molec. Struct.*, **320**, 91.
[55] Kagann, R. H., and Maki, A. G., 1983, *J. quant. Spectrosc. radiat. Transfer*, **30**, 37.
[56] Ashmore, P. G., and Tyler, B. J., 1961, *J. chem. Soc.*, 1017.
[57] Varma, R., and Curl, R. F., 1976, *J. phys. Chem.*, **80**, 402.
[58] Bongartz, A., James, K., Welter, F., and Schurath, U., 1991, *J. phys. Chem.*, **95**, 1076.
[59] Bowman, W. C., De Lucia, F. C., and Helminger, P., 1981, *J. molec. Spectrosc.*, **88**, 431.
[60] Farnell, L., and Ogilvie, J. F., 1982, *Proc. R. Soc.* A, **381**, 443.
[61] Nguyen, M. T., and Hegarty, A. F., 1984, *J. chem. Soc., Perkin Trans. II*, 2037.
[62] Murto, J., Räsänen, M., Aspiala, A., and Lotta, T., 1985, *J. molec. Struct., Theochem.*, **23**, 213.
[63] Darsey, J. A., and Thompson, D. L., 1987, *J. phys. Chem.*, **91**, 3168.
[64] Nakamura, S., Takahashi, M., Okazaki, R., and Morokuma, K., 1987, *J. Am. chem. Soc.*, **109**, 4142.
[65] Turner, A. G., 1985, *J. phys. Chem.*, **89**, 4480.
[66] Wiberg, K., 1988, *Inorg. Chem.*, **27**, 3694.
[67] Panchenko, Yu. N., De Maré, G. R., and Pupyshev, V. I., 1995, *J. phys. Chem.*, **99**, 17544; *ibid.*, **100**, 11202.
[68] Skaarup, S., and Boggs, J. E., 1976, *J. molec. Struct.*, **30**, 389.
[69] Benioff, P., Das, G., and Wahl, A. C., 1976, *J. chem. Phys.*, **64**, 710.
[70] Dargelos, A., El Ouadi, S., Leotard, D., and Chalet, M., 1977, *Chem. Phys. Lett.*, **51**, 545.
[71] Radom, L., Hehre, W. J., and Pople, J. A., 1971, *J. Am. chem. Soc.*, **93**, 289.
[72] Pople, J. A., and Gordon, M., 1967, *J. Am. chem. Soc.*, **89**, 4253.
[73] Coffin, J. M., and Pulay, P., 1991, *J. phys. Chem.*, **95**, 118.
[74] Hsu, C.-C., Lin, M. C., Mebel, A. M., and Melius, C. F., 1997, *J. phys. Chem.* A, **101**, 60.
[75] Suter, H. U., and Huber, J. R., 1989, *Chem. Phys. Lett.*, **155**, 203.
[76] Lee, T. J., and Rendell, A. P., 1991, *J. chem. Phys.*, **94**, 6229.
[77] Agrawal, P. M., Thompson, D. L., and Raff, L. M., 1995, *J. chem. Phys.*, **102**, 7000.
[78] Roothan, C. C. J., 1951, *Rev. mod. Phys.*, **23**, 69.

[79] MØLLER, C., and PLESSET, M. S., 1934, *Phys. Rev.*, **46**, 618.
[80] BECKE, A. D., 1993, *J. chem. Phys.*, **98**, 5648.
[81] BECKE, A. D., 1992, *J. chem. Phys.*, **96**, 2155.
[82] LEE, C., YANG, W., and PARR, R. G., 1988, *Phys. Rev.* B, **37**, 785.
[83] CURTISS, L. A., RAGHAVACHARI, K., TRUCKS, G. W., and POPLE, J. A., 1991, *J. chem. Phys.*, **94**, 7221.
[84] FRISCH, M. J., TRUCKS, G. W., SCHLEGEL, H. B., GILL, P. M. W., JOHNSON, B. G., ROBB, M. A., CHEESEMAN, J. R., KEITH, T., PETERSSON, G. A., MONTGOMERY, J. A., RAGHAVACHARI, K., AL-LAHAM, M. A., ZAKRZEWSKI, V. G., ORTIZ, J. V., FORESMAN, J. B., PENG, C. Y., AYALA, P. Y., CHEN, W., WONG, M. W., ANDRES, J. L., REPLOGLE, E. S., GOMPERTS, R., MARTIN, R. L., FOX, D. J., BINKLEY, J. S., DEFREES, D. J., BAKER, J., STEWART, J. P., HEAD-GORDON, M., GONZALEZ, C., and POPLE, J. A., 1995, *Gaussian 94*, *Revision B.3*, (Pittsburgh, Pennsylvania: Gaussian, Inc.).
[85] DE MARÉ, G. R., and NEISIUS, D., 1984, *J. molec. Struct., Theochem.*, **109**, 103.
[86] DE MARÉ, G. R., PANCHENKO, YU. N., and VANDER AUWERA, J., 1997, *J. phys. Chem.* A, **101**, 3998.
[87] LEE, T. J., and RICE, J. E., 1992, *J. phys. Chem.*, **96**, 650.
[88] COX, A. P., and RIVEROS, J. M., 1965, *J. chem. Phys.*, **42**, 3106.
[89] MEBEL, A. M., MOROKUMA, K., LIN, M. C., and MELIUS, C. F., 1995, *J. phys. Chem.*, **99**, 1900.
[90] FREI, H., and PIMENTEL, G. C., 1985, *A. Rev. phys. Chem.*, **36**, 491.
[91] VASSIDEV, R., and NOVICKI, S. W., 1998, *Chem. Phys.*, **226**, 201.
[92] NOVICKI, S. W., and VASSIDEV, R., 1991, *Chem. Phys. Lett.*, **176**, 118.
[93] MELEN, F., and HERMAN, M., 1992, *J. Phys. Chem. Ref. Data*, **21**, 831.
[94] JACOX, M. E., 1990, *J. Phys. Chem. Ref. Data*, **19**, 1387.
[95] HURTMANS, D., HERMAN, M., and VANDER AUWERA, J., 1993, *J. quant. Spectrosc. radiat. Transfer*, **50**, 595.